doi.org/10.36721/PJPS.2026.39.10.295.1

Formulation and evaluation of sustained-release pitavastatin-loaded chitosan nanoparticles for enhanced anti-hyperlipidemic activity

Amina Arshad[1], Muhammad Zaman[2], Humayun Riaz[1], Muhammad Sajjad Haider[3], Wafa Ishaq[4], Sherjeel Adnan[5], Zeeshan Masood[3], Hammad Ahmed[6], Nabeela Ameer[3], Hafiz Muhammad Abdur Rahman[7], Muhammad Waqas[8] and Muhammad Farooq[3]*,

[1]Rashid Latif College of Pharmacy, Lahore, Pakistan
[2]Faculty of Pharmacy, University of Central Punjab, Lahore, Pakistan
[3]School of Pharmacy, Multan University of Science and Technology, Multan, Pakistan
[4]Faculty of Pharmacy, The University of Lahore, Lahore, Pakistan
[5]Allied Institute, Multan, Pakistan
[6]Sialkot Institute of Science and Technology, Sialkot, Pakistan
[7]Southern Punjab Institute of Health Sciences, Multan, Pakistan
[8]School of Computing, Engineering and the Built Environment, Edinburgh Napier University, Edinburgh, EH10 5DT, UK

Abstract: **Background**: Pitavastatin (PVN), a BCS class-II drug, exhibits poor aqueous solubility leading to limited oral bioavailability and therapeutic efficacy. **Objectives**: This study aimed to enhance the solubility and anti-hyperlipidemic efficacy of Pitavastatin (PVN) by encapsulating it in chitosan-based polymeric nanoparticles. **Methods**: Pitavastatin-loaded chitosan nanoparticles (NPs) were prepared using the ionic gelation method. Formulations were characterized by particle size, zeta potential, drug loading, *In-vitro* drug release and surface morphology. Fourier transform infrared spectroscopy (FTIR), X-ray diffraction (XRD), thermal analysis (TGA and DSC), *ex-vivo* intestinal permeability and *in-vivo* pharmacodynamic analysis were also performed. **Results**: The size of PVN-loaded NP ranged from 219.9±1.11 to 292.7±2.29 nm with PDI 0.2-0.4, surface charge of +28.4 ± 0.43 to 32.5 ± 1.02 mV and entrapment efficiency 65±1.12-93±1.23%. Solubility in different media (PBS (pH 6.8), 0.1N HCl (pH 1.2) and distilled water showed a 56-102-fold increase compared to PVN. SEM analysis revealed a smooth surface and spherical geometry of the NP. FTIR analysis confirmed that there was no physicochemical interaction between PVN and chitosan in NP formulations (NP1-NP5). XRD and thermal analysis indicated the amorphous nature of PVN-loaded NP. *In-vitro* drug release from NP formulations (NPI-NP5) ranged from 80.97±4.80 to 81±3.90% indicating sustained release, while *ex-vivo* intestinal permeability was 1.5-fold higher than PVN. The optimized formulation (NP1) followed Higuchi release model, indicating Fickian diffusion. Pharmacodynamic analysis of lipid profiles in hyperlipidemic albino rats suggested that NP1 reduced low-density lipoprotein (LDL) by 33±1.24 %, total cholesterol by 29±2.13% and triglycerides by 23±1.21%, showing better results than PVN. **Conclusion**: Chitosan-based Pitavastatin nanoparticles successfully enhanced drug solubility and provided sustained release, leading to improved *ex-vivo* permeability and greater *in-vivo* anti-hyperlipidemic activity in albino rats. This approach represents a promising strategy for enhancing therapeutic potential of Pitavastatin.

Keywords: Anti-hyperlipidemic; Chitosan; Ionic gelation; Pitavastatin; Solubility enhancement

Submitted on 30-01-2026 – Revised on 25-02-2026 – Accepted on 25-03-2026

INTRODUCTION

Nanotechnology-based drug delivery systems, particularly polymeric nanoparticles, have emerged as a fast-growing approach for addressing these problems, as they have addressed several issues with therapeutic agents, such as low solubility, inability to target specific sites, inaccurate distribution, toxicity and a narrow therapeutic window (Wei *et al*., 2020). Additionally, nanotechnology is considered one of the most promising approaches for improving drug dissolution, solubility and bioavailability (Korani *et al*., 2019).

Chitosan, a natural cationic polymer composed of (1•4)-β-D-glucan 2-amino-2-deoxy, has attracted significant attention because of its biodegradability, pH sensitivity and biocompatibility (Wei *et al*., 2020). It also exhibits characteristics that enable it to adhere to the mucus surface and open tight junctions between epithelial cells, thereby enhancing drug absorption. Chitosan improves the bioavailability and stability of unstable drug molecules and sustains their release by increasing permeability and drug effectiveness at the nanoscale (Basso *et al*., 2025).

Hyperlipidemia is one of the major risk factors associated with cardiovascular disorders, a leading cause of morbidity and mortality worldwide. Elevated plasma cholesterol, triglycerides and low-density lipoproteins (LDL) contribute to the progression of atherosclerosis, hypertension and coronary heart disease. Pitavastatin (PVN) is an odorless, white to light yellow, crystalline,

**Corresponding author:* e-mail: farooqali10@yahoo.com

hygroscopic drug that belongs to BCS class II, i.e., possessing low aqueous solubility, low bioavailability and high permeability (Harisa *et al*., 2016). PVN, being structurally similar to HMG-CoA, binds to HMG-CoA reductase more attractively than the natural substrate (Pimple *et al*., 2022). Consequently, LDL uptake by LDL receptors from the blood into the liver is increased, thereby reducing plasma triglyceride levels (Ashfaq *et al*., 2022).
The ionic gelation method, based on the interaction between negatively charged polyanions (sodium tripolyphosphate) and positively charged chitosan, offers an efficient means of preparing nanoparticles. This approach prevents drug degradation and ensures biocompatibility. The ionic gelation method is widely adopted because it is simple, rapid and does not involve any chemical reactions, organic solvents, or high temperatures (Van Bavel *et al*., 2023).

The novelty of this work lies in its systematic multi-domain validation, demonstrating not only a significant 56-102-fold increase in solubility through amorphization but also establishing a clear correlation between sustained *In-vitro* release enhancement in *ex-vivo* intestinal permeability and superior *in-vivo* pharmacodynamic outcomes. Unlike previous reports that often focus solely on formulation optimization; this research uniquely confirms that optimized chitosan nanoparticle formulation (NP1) translates directly into a statistically significant reduction in key lipid parameters in a hyperlipidemic rat model, outperforming pure drug. By integrating detailed physicochemical analysis with robust biological performance data, this study provides a compelling proof of concept for chitosan nanoparticles as a viable, scalable platform to overcome solubility-limited bioavailability of Pitavastatin, offering a promising alternative for more effective clinical management of hyperlipidemia.

MATERIALS AND METHODS

Pitavastatin (PVN) was donated by CCL Pharmaceuticals (Pvt) Lahore Pakistan, Acetic Acid, Chitosan, Sodium tripolyphosphate (NaTPP) (Sigma Aldrich Gmb Chemie, Germany), Ethanol, Chloroform (Merck, Germany), Tween 80 (Sigma Aldrich Gmb Chemie, Germany), Distilled water was prepared in post graduate research lab of Faculty of Pharmacy, University of Lahore.

Synthesis of drug-loaded chitosan NP by the ionic gelation method

The ionic gelation method was used to prepare drug-loaded chitosan. An aqueous acetic acid solution (1% v/v) is used to prepare a final Chitosan solution concentration of 0.2% w/v. 25 mL of chitosan solution is incorporated into (10 mL) previously prepared acetic acid (1%) solution. 10 mL of chloroform, as a vehicle for 2mg PVN, is used to initiate gelation. The complexation is assisted by the addition of 12 mL sodium tripolyphosphate (0.1% w/v), positively charged sodium ions bind to oppositely charged PVN molecules. Homogenizing the mixture at 800 rpm for 15 minutes further supports the observation of complex gel formation and results in the evaporation of chloroform. Continuous stirring of the drug-gel-complexation resulted in precipitated drug-loaded nanoparticles. The drug's compatibility with chitosan is physically apparent as precipitation after centrifugation (Sarkar *et al*., 2020). Collected nanoparticles were washed with distilled water to remove any surface-adsorbed or residual solvent.

Particle size, zeta potential, essential and poly dispersity index (PDI)

PVN-loaded NP Formulations (NP1- NP5) were evaluated to check particle size, zeta potential and polydispersity index (PDI). Drug-loaded NP dispersion (10 ml) was collected by ultra-centrifugation and diluted with deionized water 1:10. Particle size, zeta potential and PDI were evaluated by using Zeta sizer (ZS-90 Malvern Instruments, UK). All calculations were measured in a triplicate manner (n=3) at 25 °C with an angle of detection (90°) (Shahid *et al*., 2022).

Entrapment efficiency

Entrapment efficiency (EE%) of the formulations was evaluated by high-shear centrifugation (Eppendorf Centrifuge 5810 R, Germany) for 30 min at 15000 rpm. The quantity of drug-loaded PVN NP incorporated in chloroform was then examined using a UV spectrophotometer (UV-1800, Japan, 240V) at 244 nm (Alehosseini *et al*., 2022). The entrapment efficiency (%EE) was estimated by following Equation 1.

$$\mathrm{EE}(\%) = \frac{\text{Weight of drug encapsulted}}{\text{Weight of total drug added}} \times 100 \text{ ------} \quad (1)$$

Where Men is the amount of drug encapsulated and Min is the drug input quantity in the processing.

Solubility analysis

Solubility measures for pure drug and NP1-NP5 are separately determined in three different environments: Phosphate Buffer Solution (PBS) (pH 6.8), 0.1 N HCl (pH 1.2) and double-distilled water. An excessive quantity of pure drug and NP1-NP5 were dispersed in 5ml Eppendorf tubes in their respective solvents and placed on a water bath shaker at 100 rpm and 37°C for 36 h. The samples were then centrifuged for 15 min at 6000 rpm. The supernatant solution was measured using a UV-1800 Spectrophotometer (Japan, 240V) at 244 nm (Ashfaq *et al*., 2022).

Scanning electron microscopy (SEM)

It is an essential technique for investigating the shape and surface morphology of NPs, even with limited size information. NP were diluted 1:10 (v/v) with deionized water and then dilutions were spotted on an aluminum disc

and dried for further analysis. The dried formulation was coated with gold using a sputter coater. Gold-coated NP formulations (NP1-NP5) were kept on a SEM (Quanta 400 ESEM/EDAX) stub at 50 mA through a sputter for 6 min (Sifaoui *et al*., 2022).

Physicochemical characterization

Fourier transform spectroscopy (FTIR) of PVN, chitosan and PVN-loaded NP was exhibited on a spectrophotometer (RF-5301PC Shimadzu, Japan). Infrared spectra of the drug, excipients and drug-loaded NP were recorded in the mid-infrared range (400-4000 cm-1) in Transmittance mode at 10 scans/min at room temperature (Mourdikoudis *et al*., 2018). XRD studies were performed to confirm the amorphous or crystalline state of the drug, polymer and drug-loaded polymer. An X-ray diffractometer (D8 Discover, Bruker, Germany) was used to record the X-ray diffractogram over a scanned range (2θ) of 4-70° at a scan rate of 1°/min. Thermal behavior of PVN, excipients and PVN-loaded NP s were conducted to evaluate any possible interaction of the drug with formulation components (Pyris diamond series, TG/DSC, Perkin Elmer, USA). Samples were placed in an aluminum crucible and heated to 0-300°C at 10°C/min under a nitrogen gas flow to create an inert atmosphere (Elsayed *et al*., 2023).

In-vitro drug release studies

To analyse drug release from PVN-loaded NP, a dialysis membrane was used. 100 mg of NP1-NP5 (containing 2 mg PVN) were dispersed in 3ml of 0.1 N HCl (pH 1.2) and PBS (pH 6.8), then transferred to a dialysis membrane (7000 KD). The dialysis bag was tightly sealed at both ends and placed in a 250 ml beaker containing 0.1 N HCl (pH 1.2) and PBS (pH 6.8), respectively, at 37°C with a stirring speed of 100 rpm. Samples (5 ml each) were taken at predetermined time intervals: initially at 30 min, then every hour until 12h. A similar volume of dissolution medium was added to the vessel to make up the volume. The amount of PVN was evaluated spectrophotometrically at 244 nm and percentage drug release was then calculated (Felimban *et al*., 2023).

Ex-vivo intestinal permeability studies

Ex-vivo permeability studies were performed using the goat intestine obtained from a local slaughterhouse. The intestinal lumen was washed with physiological solution at room temperature to remove intestinal contents. NP1-NP5 were placed in the intestinal lumen by clamping both sides with a cord clamp and then placed in a beaker containing 45 mL of PBS. Continuous stirring with a magnetic stirrer at 50 rpm was performed at room temperature and at 37°C. 200 µL samples were collected at 0, 1, 2, 3, 4, 5, 6, 7, 8, 12, 24, 48 and 72 h and diluted to 4 mL (4000 µL). The amount of sample taken was replaced with a similar quantity of fresh media. The percentage of the drug was calculated from a calibration curve using a UV-spectrophotometer (Shimadzu UV-1800, Japan) at 244 nm (Ashfaq *et al*., 2022).

In-vivo evaluation of hypolipidemic potential for pharmacodynamics analysis

To assess the pharmacodynamic potential of drug-loaded formulations, NP1-NP5 were compared with the marketed formulation PITALO® 2mg (GENIX Pharma). Albino rats of either sex with a weight range of 150 –200 g were randomly divided into eight groups, each consisting of five rats. A total of 40 animals were used in the study and were housed in the animal house under standard environmental conditions (25±1°C) with a 12 h dark/light cycle at the Faculty of Pharmacy, University of Lahore. The study protocol was approved by the Institutional Research Ethical Committee (IREC) of the University of Lahore, vide no. IREC-2020-50. Animals had easy access to water and, along with a standard ad libitum diet, except for Group 1, each group was given an HC diet (coconut oil with 2% cholesterol) for 4 weeks. Standard diet was given to the control group (Group 1), Group 2, the negative control was given filtered water throughout the experimental period, whereas the remaining six groups (3-8) were concomitantly treated with their respective drug regimen 2h after the HC diet through oral gavage as follows. Group 3, 4, 5, 6, 7 were treated with NP1, NP2, NP3, NP4 and NP5, respectively (2 mg/kg/day each). In Group 8, the marketed dosage form, PITALO 2 mg (GENIX Pharma) (2 mg/kg/day), was administered. Body weight was checked weekly, whereas other biochemical parameters were assessed at the end of 4 weeks of the study. At the end of the experimental period, the animals were anesthetized with chloroform, after doing sternotomy, cardiac puncture was done and blood was collected for performing tests (Kurakula *et al*., 2015). To prevent observer bias, a laboratory technician who was blinded to the treatment group allocation conducted all biochemical analyses. The blinding code was not broken until after all data had been collected and statistically analyzed.

Plasma lipids determination

The level of cholesterol in plasma was measured using a commercial kit (ab65390). Triglyceride (TG), High-density lipoprotein (HDL) and total cholesterol levels were determined. Low-density lipoprotein (LDL) cholesterol was calculated using the Fried Ewald formula and very low-density lipoprotein (VLDL) cholesterol was calculated using the Fried Ewald formula (Ashfaq *et al*., 2022). The Fried-Ewald formula used to estimate levels of low-density lipoprotein cholesterol (LDLC) in blood plasma is as follows:

$$\text{LDLC} = \text{Total Cholestrol} - \text{HDLC} - \left(\frac{\text{TG}}{5}\right) \quad \text{---------- (2)}$$

Where LDLC is low-density lipoprotein cholesterol (often referred to as "bad cholesterol"), TC is the total cholesterol level in the blood, HDLC is the high-density lipoprotein

cholesterol (often referred to as "good cholesterol") and TG is triglycerides (a type of fat found in the blood). This equation is typically used when triglyceride levels are less than 400 mg/dL. If triglycerides are higher, the formula may not be accurate.

Statistical analysis

All data were expressed as mean ± standard error of mean (SEM) from five independent replicates (n=5 per group). Statistical analysis was performed using One-Way Analysis of Variance (ANOVA) followed by post hoc Dunnett's multiple comparison test to compare all treatment groups against the negative control group (Katsuki *et al*., 2022). Dunnett's test was specifically chosen as it controls the Type I error rate when multiple comparisons are made against a single control group. Normality of data distribution was confirmed using Shapiro-Wilk test and homogeneity of variances was verified by Levene's test prior to ANOVA. A probability value of $p < 0.05$ was considered statistically significant, with significance levels denoted as *p<0.05, **p<0.01, ***p<0.001 and ****p<0.0001. GraphPad Prism version 5.0 was used for all statistical analyses and graphical presentations."

RESULTS

Particle size, zeta potential and polydispersity index

Zeta sizer was used to determine the average size and zeta potential of drug-loaded chitosan. NP1, NP2, NP3, NP4 and NP5 showed particle sizes of 219.9±1.11nm, 254.1± 1.09 nm, 240±1.32 nm, 263.6±2.16 nm and 292.7±2.29 nm, respectively (Table 1) (Fig. 1 A). It was observed from the results that equal concentrations of NaTPP and chitosan in NP1 produced small-sized particles 219.9±1.11 nm as compared to a lower concentration of NaTPP in NP5 (292.7±2.29). PDI results of NP1-NP5 vary in the range of 0.45-0.56, indicating a homogenous nature, greater stability and excellent dispersity of NP in solution form (Table 2) (Mourdikoudis *et al*., 2018). The charge on the surface and the rate of particle movement were measured by zeta potential. Zeta potential of NP1, NP2, NP3, NP4 and NP5 were 29.1±0.89, 32.5±1.02, 29.5±0.74, 28.7±0.85 and 28.4±0.43 mV, respectively (Fig. 1 B) (Table 2) (Ramani *et al*., 2021).

Entrapment efficiency (%)

It was observed that PVN was maximum entrapped by NP formulation NP1, i.e. 93±1.23% followed by a decreasing pattern in drug uptake in formulations NP2 towards NP5, where the uptake of PVN was the least of all, with values of 83±1.42%, 78±1.57%, 71±1.03% and 65±1.12%, respectively (Table 2).

Solubility analysis of PVN alone and PVN-loaded NP is determined separately for PBS (pH 6.8), 0.1N HCl (pH 1.2) and distilled water, as shown in Fig. 1C. The solubility of PVN was found between 0.01 ± 0.002 to 0.039 ± 0.003 µg/ml in the above solutions, indicating that PVN is poorly water-soluble. The optimal availability of sodium ions positively affects drug-gel-complexation in an ionic pattern to enhance the solubility of PVN. As the concentration of NaTPP decreased from NP1-NP5, the solubility of PVN also decreased from 4.0±0.52 µg/ml to 2.3±0.15 µg/ml (Fig. 1C). NP1 resulted in a comparatively lower solubility of 3.80±0.23 µg/mL in 0.1N HCl compared to the solubility profile in PBS.

SEM analysis

Surface morphology, along with structural characteristics of PVN-loaded NP formulations, was evaluated by scanning electron microscope. It is evident from the SEM analyses in (Fig. 2) that all the formed NP have smooth surfaces in all formulations, also falling in the nanoparticle size range as well. Particle shape was also regular from the images obtained in SEM analysis, indicating that selected ratios of chitosan and NaTPP have given smooth and regular shape. Further, regarding the PDI findings, it was assessed that all particles in each formulation have nearly uniform size distributions, indicating a very controlled NP formulation.

FTIR spectroscopy

FTIR analysis was performed to detect possible interactions among PVN, NaTPP and chitosan. FTIR spectra of PVN showed characteristic peaks at 760 cm^{-1}, 1407 cm^{-1}, 1560cm^{-1}, 2946 cm^{-1} and 3320 cm-1 that correspond to C–F group, C=C bending, C–H stretching, O–H and C=O stretching, respectively (Fig 3 A)(Ashfaq *et al*., 2022). FTIR spectra of chitosan showed bands at 1153 cm-1, 1624 cm-1 and 1666 cm-1, corresponding to asymmetric stretching of the C-O-C bridge and C-O stretching, respectively. The existence of the N-acetyl group was depicted by characteristic bands at 1320 cm-1 and 1654 cm-1 that correspond to C-N stretching of amide III and C=O stretching of amide I. Absorption bands at 2865cm^{-1} and 2984 cm^{-1} are attributed to asymmetric and symmetric C-H stretching of the polysaccharide. The strong band at 3334 cm^{-1} indicated N-H and O-H stretching behavior and intramolecular hydrogen bonding (Fig. 3A).

X-ray diffraction (XRD) analysis

XRD pattern of PVN represented sharp intense peaks at a diffraction angle (2θ) of 6.6°, 8.9°, 10.25°, 13.6°, 18.39°, 20.75°, 20.04°, 26.95°, 30.1° and their respective counts were 627, 435, 438, 635, 474, 819, 317, 291 (Fig 3B) (Pimple *et al*., 2022). Chitosan showed broad peaks at 6.5° and 20.85° and their respective counts were 346 and 357, respectively. Formulation NP1 exhibited low-intensity peaks at a diffraction angle (2θ) of 16.3°, 19.0° and 21.35° and their respective counts were 375, 391 and 376, respectively (Fig 3B). NP1 represented very low-intensity peaks at a diffraction angle (2θ) of 24.8°and 30.55° and their respective counts were 258 and 253, respectively.

Table 1: Formulation of PVN-loaded nanoparticles (NP).

Formulation code	NaTPP (mg)	Chitosan (mg)	PVN (mg)
NP1	50	50	2
NP2	40	60	2
NP3	30	70	2
NP4	20	80	2
NP5	10	90	2

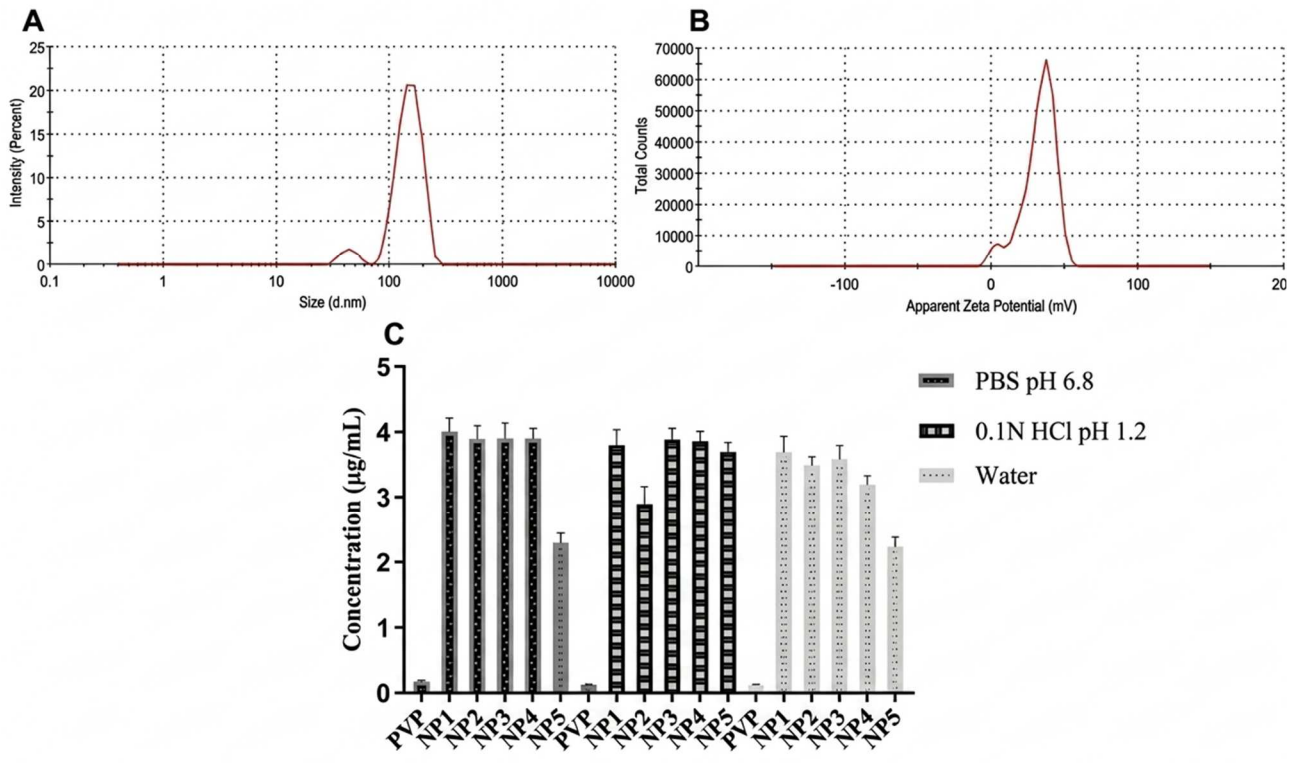

Fig. 1: Average particle size (A) zeta potential (B) and solubility analysis of PVN and NP formulations (NP1-NP5) in PBS (pH 6.8), 0.1 N HCl (pH 1.2) and distilled water (C).

Table 2: Particle size, zeta potential, polydispersity index and entrapment efficiency of developed formulations.

Formulation	Particle size (nm)	Zeta potential (mV)	PDI	Entrapment efficiency (%)
NP1	219.9 ± 1.11	29.1±0.89	0.48±1.21	93±1.23
NP2	254.1 ± 1.09	32.5±1.02	0.47±1.32	83±1.42
NP3	240.3 ± 1.32	29.5±0.74	0.45±0.87	78±1.57
NP4	263.6 ± 2.16	28.7±0.85	0.51±0.68	71±1.03
NP5	292.7 ± 2.29	28.4±0.43	0.56±1.19	65±1.12

Thermal analysis

Through Thermogravimetric analysis results, PVN showed an initial 20% loss of mass from 50-100°C, which was due to moisture content or physically absorbed water. Maximum 60% degradation of was. identified in a range of 190-400°C that corresponds to the melting of PVN and the oxidation process (Fig 3C) (Ashfaq *et al*., 2022). Chitosan showed first weight loss 10% from 40-100°C attributed to moisture loss while subsequent 80% weight loss showed in temperature range of 265-400°C due to vaporization, elimination of volatile compounds and deacetylation of chitosan (Fig. 3C). Chitosan degradation starts with formation unsaturated structure of amino group, polysaccharide randomly split into glycoside bond and formation of butyric acid, acetic acid and lower fatty acid after decomposition. NP1 followed a similar temperature

range and weight loss with a minor shift. First phase exhibited 15% loss of weight (45-90°C), while 80% loss of mass in the second phase (140-33°C). DSC thermographs of PVN showed sharp endothermic peaks at 100°C and 130°C, which were attributed to evaporation or loss of water vapors (Fig. 3D). PVN also showed endothermic peaks at 225°C and 240°C that correspond to the melting of the drug (Pimple *et al*., 2022). Chitosan exhibited an endothermic peak at 100°C, which was due to dehydration or loss of water related to the hydrophilic group of the polymer. Polysaccharides of chitosan have an affinity with water and a disordered structure. NP1 depicted a wide endothermic peak at 90°C that represented the evaporation of moisture content in the formulation (Fig. 3D). NP1 does not exhibit any sharp peaks that indicate the complete PVN encapsulation into chitosan.

In-vitro drug release

The *in-vitro* dissolution of PVN-loaded NP formulations was determined by drug release in 0.1 N HCl, pH 1.2 and pH 6.8 at 37°C. NP2, NP3, NP4 and NP5 delineated similar patterns of drug release and did not show significant differences from each other. PVN released from all formulations showed respective cumulative release of 13, 10, 9 and 8% for initial 2h in 0.1N HCl (pH 1.2), while NP1 showed a significant difference in drug release (19%) (Fig. 4A). Herein, at the initial 30 min, there was also seen abrupt drug release (7% release) indicating there was small quantity of PVN adsorbed on NP surface. The release pattern of PVN from NP displayed a biphasic profile, with an initial burst release of up to 20%, followed by sustained release over 12h, likely due to diffusion or erosion of the drug from the polymer matrix. NP1 surpassed in releasing significantly more PVN (81%) as compared to that released from NP2, NP3, NP4 and NP5, with drug release of 61%, 60%, 51% and 53%, respectively (Fig. 4B) (Delwar *et al*., 2023). The PVN release from the nanoparticle in PBS (pH 6.8) was much faster than in an acidic medium (pH 1.2).

Drug release kinetics

Different kinetic models, including Zero-order, first-order, Higuchi, Korsmeyer Peppas, evaluated drug release from NP and Hixon Crowell by applying MS Excel (DD solver). NP1, NP2, NP3 and NP4 followed the Higuchi release model with the highest linearity (R2 = 0.9016-0.9792), explaining the drug release from NP, as NP as a square root of time-dependent process by Fickian diffusion (Table 3). NP5 exhibited a linear relationship showing concentration-dependent release of PVN following zero-order kinetics. The release exponent (n) in the Korsmeyer-Peppas model best explained the first 60% of drug release from NP formulations. The release exponent (n) of NP1 and NP2 were 040 and 0.42, respectively, which illuminated. Fickian diffusion. NP3 and NP4 were 0.51 and 0.61, respectively, indicating non-Fickian diffusion with anomalous release, which explained the coupling of the diffusion and erosion mechanisms (Table 3) (Basso *et al*., 2025). NP5 showed an 'n' value of 0.96, which indicates a case-II transport mechanism. Case II transport illustrated the drug release mechanism associated with polymer stress and state transitions that occur when the polymer swells in biological liquids or water. Case II mechanism is dominated by polymer erosion and disentanglement (Elsayed *et al*., 2023).

Ex-vivo permeability studies

Optimized formulation NP1 exhibited the highest intestinal permeability, while NP1, NP2, NP3, NP4 and NP5 depicted intestinal permeation 76%, 59%, 57%, 56% and 50%, respectively, after 12 h (Fig. 4C). PVN showed no solid particulates and maximum solubility in intestinal medium.

Plasma lipoprotein analysis for pharmacodynamics study

Pharmacodynamics has been conducted to assess the anti-hyperlipidemic effect of the developed formulations and to compare the various hyperlipidemic parameters. Rats were dissected after 8-10 h of fasting. Various parameters, including HDL, total plasma cholesterol, triglycerides and VLDL, were calculated from the blood samples using commercial enzymatic assays. HDL, VLDL and cholesterol levels showed a non-significant increase compared with the negative control group, whereas the triglyceride levels of all treated groups showed a significant ($p < 0.0001$) increase (Table 4). Triglyceride exhibited an extremely significant ($p<0.001$) result. VLDL and HDL displayed non-significant effects. The statistical parameters of these results are given in table 5.

DISCUSSION

The ratio between chitosan and NaTPP is critical. When NaTPP is the limiting reagent (lower concentration relative to chitosan), there are insufficient anions to instantly cross-link all available chitosan cations. Similar results of ticagrelor-loaded chitosan NP were presented by Nariman Shahid *et al*., 2022 (Shahid *et al*., 2022). The lower PDI value of formulated NP indicated a narrow size distribution, suggesting equal distribution of drug within polymeric material and good uniformity in particle size. Values slightly above threshold can be justified by inherent variability of ionic gelation process at definite chitosan-TPP ratios, providing colloidal stability remains high enough to avoid aggregation. The surface charge provides greater stability to the NP by preventing particle aggregation. NP with a surface potential greater than 20 mV exhibited high colloidal stability, slow sedimentation and minimal aggregation (Ashfaq *et al*., 2022).

Drug entrapment efficiency decreases due to the polyelectrovalent capacity of NaTPP for drug molecules, leading to enhanced gel-complexation and decreased crosslinking density (Mahmoud *et al*., 2025).

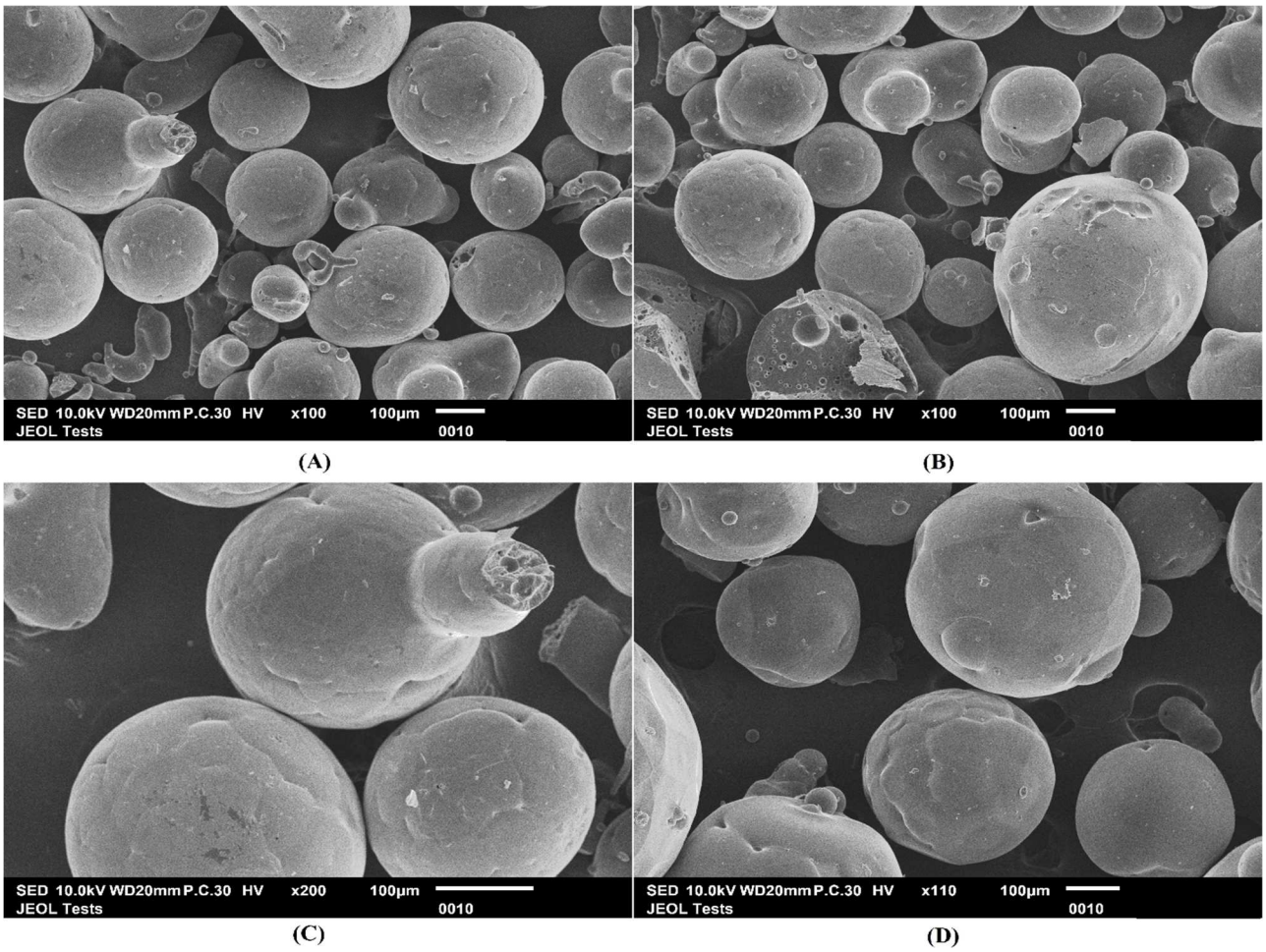

Fig. 2: Scanning electron micrographs of formulations (A and C) NP1and (B and D) NP3.

Polyelectrovalent capacity refers to its multiple negative charges, which electrostatically bind to the protonated amine groups of chitosan. When NaTPP was added, probability of instantaneous and intense interaction between chitosan and TPP increases dramatically. An excess of polymer chains leads to uncontrolled, instantaneous interaction with NaTPP, causing aggregation and precipitation. These loose aggregates lessen Vander Waal forces, which ultimately reduces the entrapment efficiency of PVN (Li *et al*., 2017). Solubility enhancement in PBS (pH 6.8), 0.1N HCl (pH 1.2) and distilled water was observed, ranging from 56-to 102-fold. Enhanced Solubility of NP1 is related to the hydrophilic nature of the cross-linking agent, enhanced dissolution rate and particle size of NP (Farooq *et al*., 2020). NP1 and NP3 showed smooth, spherical morphology with uniform size, which is beneficial for drug delivery as it ensures colloidal stability, improved interaction with the muscular surface and more accurate PVN diffusion and its release kinetics (Hadidi *et al*., 2020). Formulated NP depicted prominent peaks of PVN at 2946 cm^{-1} and 3320 cm^{-1} due to O–H and C=O stretching, respectively. The characteristic peaks of the drug at (760 cm-1, 1407 cm-1, 1560cm-1) due to the C–F group, C=C bending and C–H stretching showed a reduction in the sharpness of peaks in the drug loading, which revealed no polymer-drug incompatibility. A slight shift in the peaks did not reveal any prominent interaction between the PVN and the polymer in the formulations. NP1-NP5 exhibited a reduction in counts and sharpness of peaks as compared to PVN, which describes the reduction in crystalline behavior of the drug in formulation. Sharp and intense drug peaks at a diffraction angle (2θ) of 13.6° and 20.75° did not appear in formulations, which confirmed the amorphous nature of the drug. In the optimized formulation (NP1), the PVN endotherm was well conserved, with only minor changes in broadness and a slight shift in the temperature range. It was determined that excipients and polymeric material can affect the PVN melting endotherm with slight variations and cannot present possible incompatibility between drug and polymer. These thermographs also confirmed that there is no interaction in the melting peaks of all excipients in the mixture, which were well preserved. Hence, it is suggested that the optimized formulation (NP1) is heat-stable and can protect the drug from thermal degradation up to a certain limit.

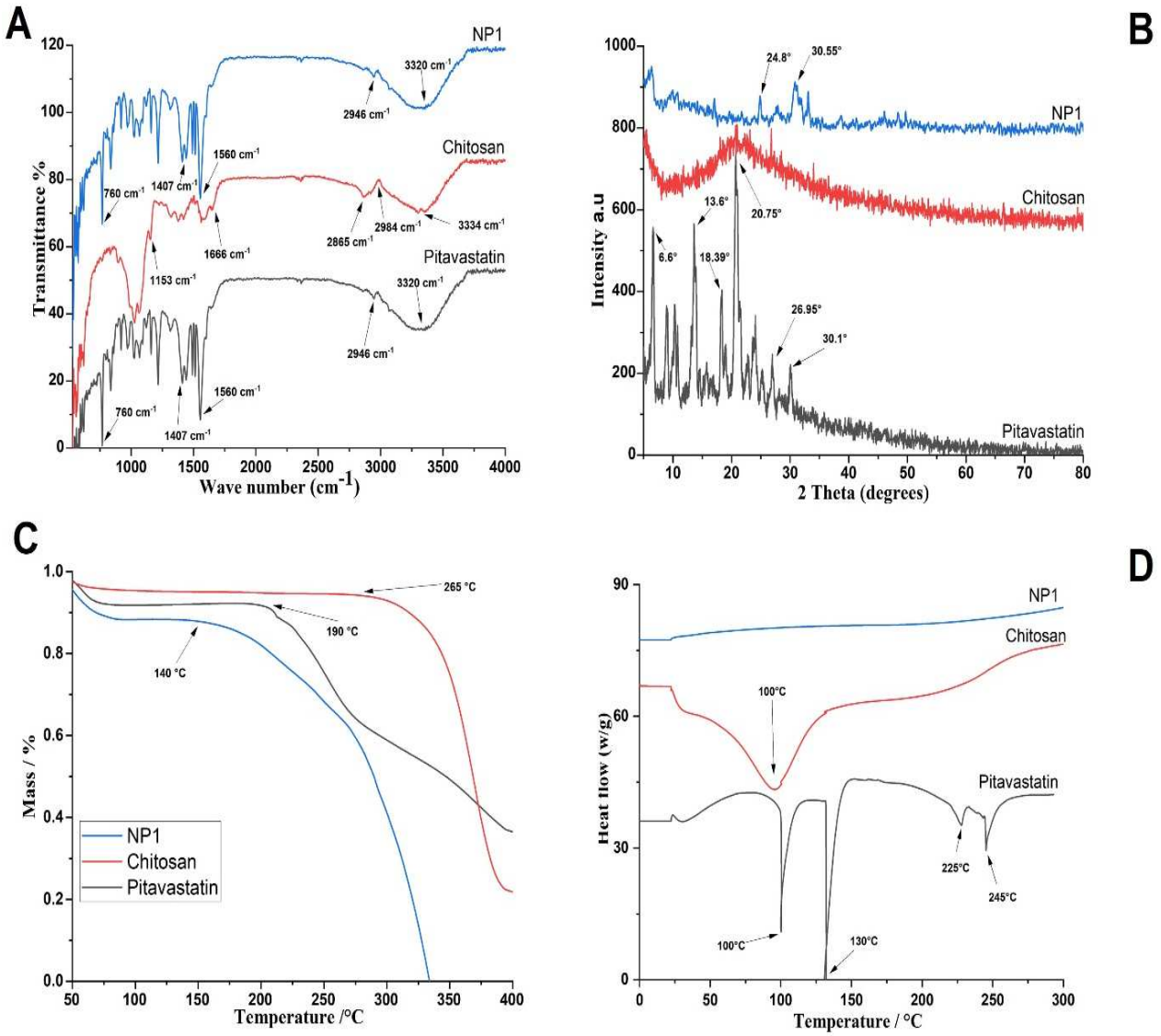

Fig. 3: (A) FTIR spectra, (B) X-ray diffractogram, (C) TGA and (D) DSC thermograms of PVN, chitosan and formulation NP1.

Table 3: Values of drug release kinetics of PVN-loaded NP.

Kinetic models		NP1	NP2	NP3	NP4	NP5
Zero order	R2	0.122	0.220	0.810	0.638	0.976
First order	R2	0.792	0.689	0.936	0.790	0.959
Higuchi model	R2	0.901	0.927	0.944	0.979	0.820
Korsemyer	R2	0.934	0.949	0.969	0.979	0.977
peppas	N	0.40	0.42	0.61	0.51	0.96

The possible reason for slow drug release was due to chitosan swelling and the adsorption behavior of NP in an acidic medium (Trucillo, 2022). This sustained release of the drug is possibly supportive for prolonged circulation of NP in systemic circulation, which enhances the bioavailability of PVN. Drug release from nanoparticle formulations was briefed as follows. Drug pka, dissolution and pH values were expected to affect the drug release behavior. Crosslinking reduction at high pH positively charged amino group (NH_3) of chitosan converted into the unionized state and drug release due to electrostatic interaction between chitosan and anions. Swelling of chitosan NP may increase in a phosphate buffer, which allows dissolution media to penetrate deeply into the polymer matrix by converting the glass polymeric material into a rubber state.

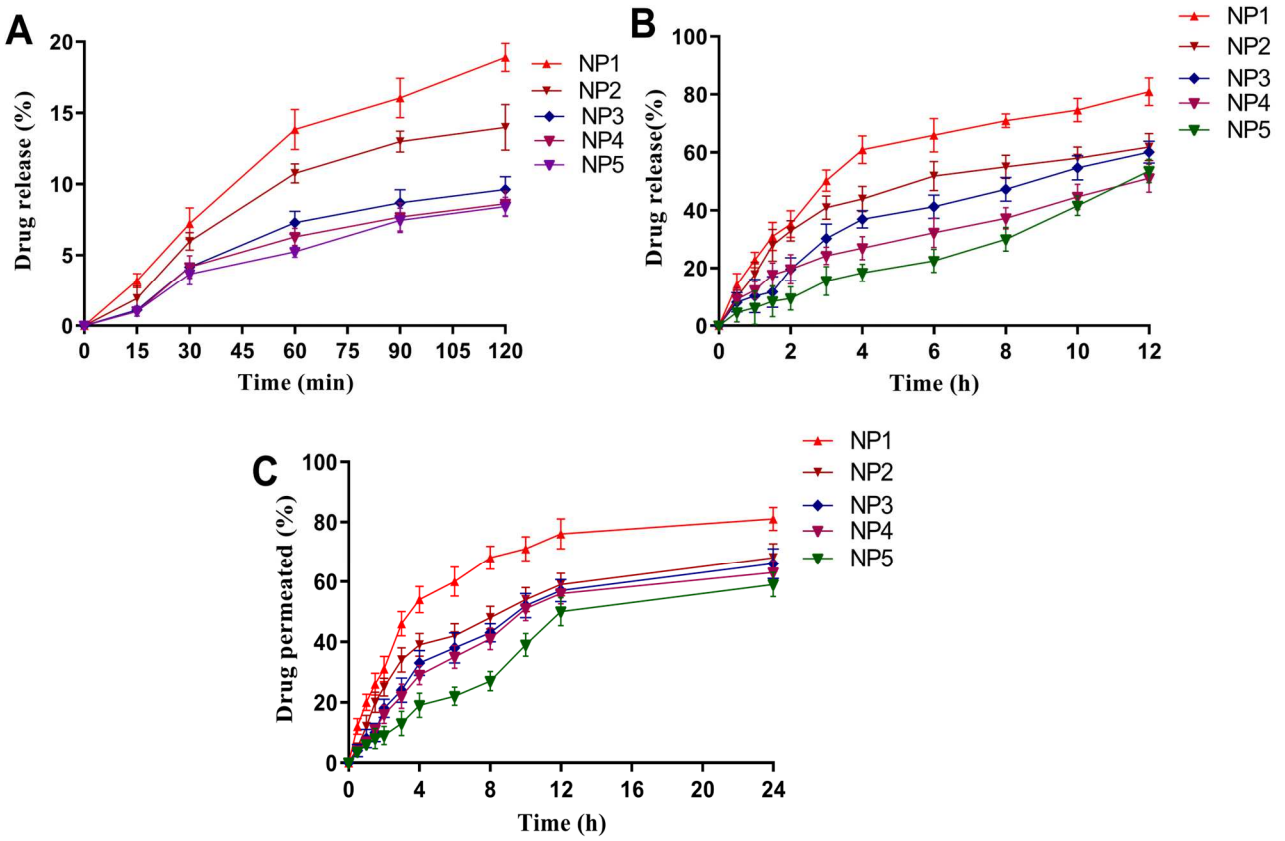

Fig. 4: (A) Drug release profile of NP1-NP5 in 0.1 N NaCl (pH 1.2), (B) PBS (pH 6.8) and (C) intestinal permeability of NP1-NP5 in PBS (pH 6.8).

Table 4: Plasma cholesterol and lipid profile of developed formulations and marketed product.

Parameters calculated	Group 1 Normal group	Group 2 Negative control	Group 3 NP1	Group 4 NP2	Group 5 NP3	Group 6 NP4	Group 7 NP5	Group 8 PITALO®
Cholesterol (mg/dl)	54.33 ± 8.66	74.667 ± 5.77***	53.33 ± 4.61**	60.21 ± 10.25**	58.66 ± 7.57**	54.66± 3.21**	57.45 ± 1.23**	52.21 ± 3.10**
HDL (mg/dl)	43.33 ± 8.08	21.667 ± 3.21****	36.00 ± 3.60**	45.2 ± 21.40**	24.00 ± 3.46 ***	26.33 ± 3.05***	42.21 ± 1.23ns	42.24 ± 3.26 ns
VLDL (mg/dl)	25.333 ± 1.15	33.667 ± 6.02***	24.666 ± 1.04 ns	27.844 ± 2.50*	23.666± 1.73 *	23.633 ± 0.57 *	24.56 ± 1.21*	23.254 ± 2.15*
Triglyceride (mg/dl)	107.66 ± 5.77	138 ± 30.19***	106.40 ± 6.55ns	96 ± 1.45*	96.66 ± 9.86**	93.00 ± 1.00**	95 ± 1.50**	108 ± 6.25ns
LDL (mg/dl)	115 ± 9.53	165 ± 4.52****	110 ± 4.61*	118 ± 3.24*	122 ± 3.45**	128 ± 2.53**	124 ± 2.67**	128 ± 1.44**

Where P value was appeared by P<0.05 *: P<0.01** and P<0.001***: P<0.0001****

Table 5: Statistical analysis of plasma lipid parameters p-values for comparisons with Normal Control (Group 1).

Parameters	Group 2 (Negative control)	Group 3 (NP1)	Group 4 (NP2)	Group 5 (NP3)	Group 6 (NP4)	Group 7 (NP5)	Group 8 (PITALO®)
Cholesterol (mg/dl)	0.0008	0.892	0.342	0.467	0.956	0.512	0.674
HDL (mg/dl)	< 0.0001	0.124	0.789	0.0005	0.0003	0.823	0.845
VLDL (mg/dl)	0.0009	0.678	0.089	0.234	0.198	0.567	0.178
Triglyceride (mg/dl)	0.0007	0.876	0.056	0.089	0.062	0.073	0.945
LDL (mg/dl)	< 0.0001	0.342	0.567	0.178	0.023	0.234	0.089

The mechanism of drug release from drug-loaded chitosan NPs involved the release of entrapped drug from the nanoparticle surface, diffusion of drug through the swollen rubber matrix and polymeric hydrolysis, erosion and breakdown, resulting in extended drug release (Herdiana *et al*., 2021). Enhanced intestinal permeability of PVN-loaded NP was due to maximum penetration, increased diffusion and the formulation's nanosized, large surface area, which could improve drug absorption. Moreover, optimized formulation NP1 has maximum solubility, which increases the drug permeation through the intestinal sac. Mehran Ashfaq *et al*. 2022 exhibited similar intestinal permeation results of Pitavastatin-loaded SNEDDS formulation (Ashfaq *et al*., 2022). NP1 had a comparable result compared to the normal group. The optimized chitosan nanoparticles (NP1) demonstrated increase in solubility due to their hydrophilic nature, small particle size and enhanced dissolution rate. This improved solubility, combined with the pH-sensitive swelling and erosion of the chitosan matrix, facilitated a sustained drug release profile conducive to prolonged systemic circulation. The resulting high concentration gradient across the intestinal membrane subsequently enhanced drug permeability and absorption. This cascade of improved biopharmaceutical properties ultimately translated into superior pharmacodynamic efficacy, with NP1 significantly improving lipid parameters to normal levels without any signs of toxicity. Thus, the chitosan-NaTPP nanoparticle system effectively bridges the gap between enhanced physicochemical properties and improved therapeutic outcomes for PVN.

CONCLUSION

Chitosan nanoparticles loaded with PVN prepared by the ionic gelation process provided better size reduction, high drug loading and cost effectiveness. PVN-loaded NP formulations showed markedly higher solubility than the pure drug. SEM analysis revealed a smooth, spherical surface of the NP, which contributed to good colloidal stability, enhanced mucosal adhesion and efficient drug delivery. FTIR, XRD, DSC and TGA results confirmed the absence of physicochemical interactions among the drug (PVN), the polymer (chitosan) and the excipients. *In-vitro* drug release and *ex-vivo* intestinal permeability studies of NP1 demonstrated more than 80% drug permeation in 24 hours. It was concluded that the development of chitosan nanoparticles could be an effective strategy for sustained release, with improved drug solubility, large surface area, favorable morphology, enhanced drug diffusion and mucosal permeation. Moreover, exploring patient-compliant dosage forms of poorly soluble drugs may further enhance this nanoparticle-based approach and its clinical potential in the management of hyperlipidemia.

Study limitations

These limitations include use of an animal model, which may not fully replicate human physiological responses, thereby limiting direct clinical translation. Potential sources of bias, including biological variability and experimental handling, despite efforts to standardize procedures. The exploratory nature of the study, which necessitates further validation through larger, well-powered studies.

Acknowledgments

The authors are grateful for the provision of research facilities at the Faculty of Pharmacy, University of Lahore, Lahore.

Author's contributions

Supervision: M F, M Z; Conceptualization: A A, M F; Methodology: S A, Z M; Validation: W I, M W; Investigation: H R, H M A; Data curation: H A, N A; Writing, Review and Editing: M S H. All authors have read and agreed to the final published version of the manuscript.

Funding

The authors have no financial funding for the completion of this project.

Data availability statement

All data analyzed during this study are included in this published article

Ethical approval

The study protocol was reviewed and approved by Institutional Research Ethical Committee (IREC) of Faculty of Pharmacy, University of Lahore, Pakistan with approval number (IREC-2020-50). This study was performed in adherence with the ARRIVE guidelines. See supplementary file for the ARRIVE checklist.

Conflict of interest

The authors declare no relevant financial or non-financial interests.

Supplementary data

https://www.pjps.pk/uploads/2026/07/SUP1784209908.pdf

REFERENCES

Alehosseini E, Shahiri Tabarestani H, Kharazmi MS and Jafari SM (2022). Physicochemical, thermal and morphological properties of chitosan nanoparticles produced by ionic gelation. *Foods.,* **11**(23): 3841.

Ashfaq M, Shah S, Rasul A, Hanif M, Khan HU, Khames A, Abdelgawad MA, Ghoneim MM, Ali MY and Abourehab MA (2022). Enhancement of the solubility and bioavailability of pitavastatin through a self-nanoemulsifying drug delivery system (SNEDDS). *Pharmceutics.,* **14**(3): 482.

Basso J, Fortuna A, Vitorino R and Vitorino C (2025). Old drugs, new tricks: Delivering pitavastatin-loaded nanostructured lipid carriers for glioblastoma treatment. *Colloids. Surf. B: Biointer.,* **245**: 114253.

Delwar S, Islam S, Al Mamun ME, Akter N and Dewan I (2023). *In-vitro* and *ex-vivo* analysis of pitavastatin-loaded liposomes for the treatment of hyperlipidemia. *Dhaka. Uni. J. Pharm. Sci.,* **22**(1): 43-54.

Elsayed SI, Girgis GN and El-Dahan MS (2023). Formulation and evaluation of Pravastatin sodium-loaded PLGA nanoparticles: *In-vitro in-vivo* studies assessment. *Int. J. Nanomed.*,**18**: 721-742.

Farooq MA, Xu L, Aquib M, Ahsan A, Baig MMFA and Wang B (2020). Denatured food protein-coated nanosuspension: A promising approach for anticancer delivery of hydrophobic drug. *J. Mol. Liq.,* **303**:112690

Felimban RI, Tayeb HH, Chaudhary AG, Felemban MA, Alnadwi FH, Ali SA, Alblowi JA, Alfayez E, Bukhary D and Alissa M (2023). Utilization of a nanostructured lipid carrier encapsulating pitavastatin–Pinus densiflora oil for enhancing cytotoxicity against the gingival carcinoma HGF-1 cell line. *Drug. Deliv.,* **30**(1): 83-96.

Hadidi M, Pouramin S, Adinepour F, Haghani S and Jafari SM (2020). Chitosan nanoparticles loaded with clove essential oil: Characterization, antioxidant and antibacterial activities. *Carbohydr. polym.,* **236**: 116075.

Harisa GI, Badran MM, Alqahtani SA, Alanazi FK and Attia SM (2016). Pravastatin chitosan nanogels-loaded erythrocytes as a new delivery strategy for targeting liver cancer. *Saudi Pharm. J.,* **24**(1): 74-81.

Herdiana Y, Wathoni N, Shamsuddin S and Muchtaridi M (2021). Drug release study of the chitosan-based nanoparticles. *Heliyon.,* **8**(1):e08674.

Katsuki S, Koga JI, Matoba T, Umezu R, Nakashiro S, Nakano K, Tsutsui H and Egashira K (2022). Nanoparticle-mediated delivery of pitavastatin to monocytes/macrophages inhibits angiotensin II-induced abdominal aortic aneurysm formation in apoe−/− mice. *J. Atherosclerosis. thrombosis.,* **29**(1): 111-125.

Korani S, Korani M, Bahrami S, Johnston TP, Butler AE, Banach M and Sahebkar A (2019). Application of nanotechnology to improve the therapeutic benefits of statins. *Drug. Discov. Today.,* **24**(2): 567-574.

Kurakula M, El-Helw A, Sobahi TR and Abdelaal MY (2015). Chitosan based atorvastatin nanocrystals: Effect of cationic charge on particle size, formulation stability and *in-vivo* efficacy. *Int. J. Nanomed.,***10**: 321-334

Li Q, Cai T, Huang Y, Xia X, Cole S and Cai Y (2017). A review of the structure, preparation and application of NLCs, PNPs and PLNs. *Nanomaterials.,* **7**(6): 122.

Mahmoud TM, Abdelfatah MM, Omar MM, Hasan OA, Wali SM, El-Mofty MS, Ewees MG, Salem AE, Abd-El-Galil TI and Mahmoud DM (2025). Enhancing the therapeutic effect and bioavailability of irradiated silver nanoparticle-capped chitosan-coated rosuvastatin calcium nanovesicles for the treatment of liver cancer. *Pharmaceutics.,* **17**(1): 72.

Mourdikoudis S, Pallares RM and Thanh NTK (2018). Characterization techniques for nanoparticles: Comparison and complementarity upon studying nanoparticle properties. *Nanoscale.,* **10**: 12871-12934.

Pimple P, Singh P, Prabhu A and Gupta S (2022). Development and optimization of HP-β-CD inclusion complex-based fast orally disintegrating tablet of pitavastatin calcium. *J. Pharm. Innov.,* **17**: 993-1010.

Ramani VD, Jani GK and Sailor GU (2021). Application of Plackett-Burman design for screening of factors affecting pitavastatin nanoparticle formulation development. *Folia. medica.,* **63**(5): 775-785.

Sarkar S, Das D, Dutta P, Kalita J, Wann SB and Manna P (2020). Chitosan: A promising therapeutic agent and effective drug delivery system in managing diabetes mellitus. *Carbohydr. Polym.,* **247**: 116594.

Shahid N, Erum A, Zaman M, Tulain UR, Shoaib QUA, Malik NS, Kausar R, Rashid A and Rehman U (2022). Synthesis and evaluation of chitosan based controlled release nanoparticles for the delivery of ticagrelor. *Des. Monomers. Polym.,* **25**(1): 55-63.

Sifaoui I, Diaz-Rodriguez P, Rodriguez-Exposito RL, Reyes-Batlle M, Lopez-Arencibia A, Villatoro LS, Castelan-Ramirez I, Omana-Molina M, Oliva A and Pinero JE (2022). Pitavastatin loaded nanoparticles: A suitable ophthalmic treatment for Acanthamoeba Keratitis inducing cell death and autophagy in Acanthamoeba polyphaga. *Euro. J. Pharm. Biopharm.,* **180**: 11-22.

Trucillo P (2022). Drug carriers: A review on the most used mathematical models for drug release. *Process.,* **10**(6): 1094.

Van Bavel N, Issler T, Pang L, Anikovskiy M and Prenner E (2023). A simple method for synthesis of chitosan nanoparticles with ionic gelation and homogenization. *Molecules.,* **28**(11): 4328.

Wei S, Ching YC and Chuah CH (2020). Synthesis of chitosan aerogels as promising carriers for drug delivery: A review. *Carbohydr. polym.,* **231**: 115744.